WATER RESOURCES RESEARCH, VOL. 49, 3747–3755, doi:10.1002/wrcr.20311, 2013

Monitoring water stable isotopic composition in soils using gas-permeable tubing and infrared laser absorption spectroscopy

Youri Rothfuss,[1] Harry Vereecken,[1] and Nicolas Brüggemann[1]

Received 29 November 2012; revised 25 April 2013; accepted 15 May 2013; published 21 June 2013.

[1] In soils, the isotopic composition of water (δ^2H and δ^{18}O) provides qualitative (e.g., location of the evaporation front) and quantitative (e.g., evaporation flux and root water uptake depths) information. However, the main disadvantage of the isotope methodology is that contrary to other soil state variables that can be monitored over long time periods, δ^2H and δ^{18}O are typically analyzed following destructive sampling. Here we present a nondestructive method for monitoring soil liquid water δ^2H and δ^{18}O over a wide range of water availability conditions and temperatures by sampling water vapor equilibrated with soil water using gas-permeable polypropylene tubing and a cavity ring-down laser absorption spectrometer. By analyzing water vapor δ^2H and δ^{18}O sampled with the tubing from a fine sand for temperatures ranging between 8°C and 24°C, we demonstrate that our new method is capable of monitoring δ^2H and δ^{18}O in soils online with high precision and after calibration, also with high accuracy. Our sampling protocol enabled detecting changes of δ^2H and δ^{18}O following nonfractionating addition and removal of liquid water and water vapor of different isotopic compositions. Finally, the time needed for the tubing to monitor these changes is compatible with the observed variations of δ^2H and δ^{18}O in soils under natural conditions.

Citation: Rothfuss, Y., H. Vereecken, and N. Brüggemann (2013), Monitoring water stable isotopic composition in soils using gas-permeable tubing and infrared laser absorption spectroscopy, *Water Resour. Res.*, *49*, 3747–3755, doi:10.1002/wrcr.20311.

1. Introduction

[2] The water stable isotopologues $^1H^2H^{16}O$ and $^1H_2{}^{18}O$ are powerful tracers of processes occurring in nature [*Yakir and Sternberg*, 2000]. Their slightly different masses as compared to the most abundant water isotopologue ($^1H_2{}^{16}O$) affect their thermodynamic (e.g., during chemical equilibrium reactions or physical phase transitions with equilibration) [*Horita and Wesolowski*, 1994; *Majoube*, 1971] and kinetic (liquid and vapor phase transport processes and chemical reactions without equilibration) properties [*Luz et al*., 2009]. This results in measurable differences in the isotopic composition of water within or between the different terrestrial ecosystem compartments (i.e., soil, groundwater, surface water, plant, and atmosphere). These differences can help to address a number of issues, among them water balance closure and flux partitioning from the soil-plant-atmosphere continuum [*Rothfuss et al*., 2010] to the field [*Williams et al*., 2004; *Yepez et al*., 2003, 2005] and regional scales [*Martinelli et al*., 1996; *Moreira et al*., 1997].

[3] Particularly in soils the isotopic composition of water provides qualitative information about whether water has only infiltrated or has already reevaporated since the last rainfall event, or about the location of the evaporation front. From water stable isotope profiles measured in soils, it is also possible, under certain assumptions, to derive quantitative information such as soil evaporation flux [*Rothfuss et al*., 2010] and the identification of root water uptake depths [*Wang et al*., 2010]. In addition, the fate and dynamics of water stable isotopologues have been well implemented into physically based soil-vegetation-atmosphere transfer models (e.g., SiSPAT-Isotope [*Rothfuss et al*., 2012], Soil-Litter-Iso [*Haverd and Cuntz*, 2010], and TOUGHREACT [*Singleton et al*., 2004]) and have demonstrated their potential.

[4] However, the main disadvantage of the use of stable isotopes in soil water studies is that contrary to other state variables (e.g., water content and tension) that can be monitored over long periods (e.g., by time-domain reflectometry, capacitive sensing, tensiometry, or micropsychrometry), stable isotopic compositions are analyzed following destructive sampling and thus are available only at a given time. As a consequence, there are important discrepancies in time resolution between soil water and stable isotope information which greatly limit the insight potential of the latter.

[5] Recently, a novel technique based on direct infrared laser absorption spectroscopy was developed that allows simultaneous and direct measurements of $^1H_2{}^{16}O$, $^1H^2H^{16}O$, and $^1H_2{}^{18}O$ mixing ratios in water vapor, which constitutes a major breakthrough in stable isotope analysis [*Helliker*

[1]Forschungszentrum Jülich GmbH, Institute of Bio- and Geosciences, Agrosphere Institute (IBG-3), Leo-Brandt-Straße Juelich, Germany.

Corresponding author: Y. Rothfuss, Forschungszentrum Jülich GmbH, Institute of Bio- and Geosciences, Agrosphere Institute (IBG-3), Leo-Brandt-Straße, Juelich D-52425, Germany. (y.rothfuss@fz-juelich.de)

0043-1397/13/10.1002/wrcr.20311

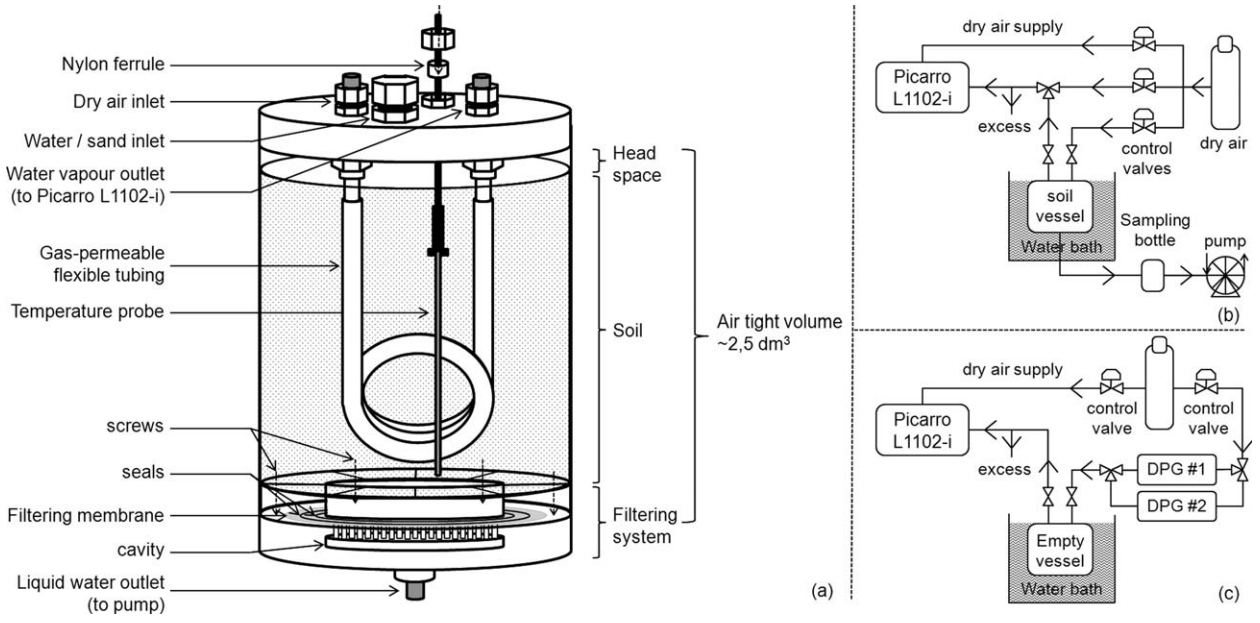

Figure 1. (a) Airtight acrylic vessel; (b) experimental setup for sampling water vapor from the vessel during calibration and withdrawing water from the soil via the vessel filtering system; and (c) experimental setup for the vapor phase tests (DPG stands for dew point generator).

and Noone, 2010; *Kerstel et al*., 1999]. Many applications can be found in the literature for varying temporal and spatial scales in the fields of hydrology [*Berman et al*., 2009; *Herbstritt et al*., 2012], boundary-layer meteorology [*Griffis et al*., 2010; *Iannone et al*., 2010], and upper-troposphere meteorology [*Webster and Heymsfield*, 2003].

[6] In this study, we present for the first time a simple methodology for monitoring soil liquid water stable isotopic composition in a nondestructive manner by sampling and measuring water vapor equilibrated with soil water, using gas-permeable polypropylene tubing and a cavity ring-down laser absorption spectrometer. We will first give a detailed description of our controlled experimental setup and water vapor sampling protocol. We will then show that following calibration in water-saturated fine sand, it is possible to track the changes of isotopic composition of soil water over a wide range of water contents and temperatures nondestructively with high time resolution.

2. Materials and Methods

[7] In the following, hydrogen and oxygen isotopic compositions of water will be expressed in per mil (‰) on the international "delta" scale as defined by *Gonfiantini* [1978] and referred to as δ^2H and δ^{18}O, respectively. Subscripts "vap" and "liq" refer to water vapor and liquid water isotopic compositions, respectively. Isotopic analysis of liquid water and water vapor was performed using a cavity ring-down spectrometer (L1102-*i*, Picarro, Inc., CA, USA) calibrated against the international primary water isotope standards V-SMOW, GISP, and SLAP by liquid water injection into the vaporizer of the analyzer.

2.1. Gas-Permeable Tubing

[8] A microporous polypropylene tubing (Accurel® PP V8/2HF, Membrana GmbH, Germany; 1 m length, 0.155 cm wall thickness, 0.55 cm i.d., 0.86 cm o.d.) was used as gas-permeable material in this study. The tubing offers the two advantages of being gas permeable (pore size of 0.2 μm) and exhibiting strong hydrophobic properties. The main purpose of this material is microfiltration, but it has also been used in environmental studies for sampling soil CO_2, N_2O, and CH_4 [*Dinsmore et al*., 2009; *Hartmann et al*., 2011; *Neftel et al*., 2000].

2.2. Experimental Vessels

[9] The experiments were performed in three airtight acrylic glass cylinders (diameter = 12.2 cm, height = 22 cm, Figure 1a) with a volume of 2.57 L. Each of these cylinders had four connecting ports at the top: one inlet for the carrier gas, i.e., synthetic dry air (20.5% O_2 in N_2 with approximately 20–30 ppmv water vapor, Air Liquide, Germany), one sample air outlet, one duct for a temperature thermistor probe (PB-5002, Gemini Data Loggers, Germany), and one access for filling the vessel with sand. All ports were sealed gastight during the measurements. Gas inlet and outlet were connected to the Accurel tubing using stainless steel end connections for flexible pipes (Swagelok, USA). The upper part of the vessel's bottom plate was perforated with 2 mm holes and covered with a water permeable Nylon® membrane (diameter = 9 cm; pore size = 0.45 μm; Whatman, UK). The set of holes ended in a 6 cm^3 cavity underneath the perforated bottom plate which had a single outlet at the bottom side of the vessel (Figure 1a). This design enabled applying a suction down to ~100 kPa for withdrawing water from the vessel using a diaphragm vacuum pump (Laboport N820.3FTP, KNF Neuberger, Germany).

2.3. Protocol for Sand Water Vapor Sampling and δ^2H and δ^{18}O Measurements

[10] For the preparation of the experiments, the vessel was filled with 0.53 L of water. The vessel's cover (with

temperature probe and a 1 m piece of gas-permeable tubing) was then placed on top of the vessel and sealed. Then, 1.4 L of sand was slowly added through the hole in the top lid, resulting in water saturation of the sand inside the vessel (corresponding to a volumetric water content of 0.38 m^3 m^{-3}; for other retention properties, please refer to *Lambot et al*. [2009]). Water vapor sampling and isotope measurements were done in the following manner: (i) dry synthetic air at a flow rate of 25 mL min^{-1} was directed through the permeable tubing; (ii) in order to reach a constant water vapor mixing ratio of 17,000 (±170) ppmv the collected water vapor was carefully diluted afterward using a mass flow controller (El Flow, Bronkhorst, Netherlands) with a flow of dry synthetic air depending on the original concentration of the sample air. Setting water vapor mixing ratio to 17,000 (±170) ppmv allowed to eliminate the dependencies of δ^2H and δ^{18}O values on water vapor mixing ratios as investigated by *Schmidt et al*. [2010]. The combined flow (original water vapor and additional dry air) was sufficient to provide an excess flow (~25–30 mL min^{-1}, depending on sand temperature) to the analyzer (Figure 1b) in order to avoid any contamination of sample air with ambient air. (iii) After δ^2H and δ^{18}O had reached steady values (standard deviations <0.7‰ and <0.2‰ for δ^2H and δ^{18}O, respectively) for a period of approximately 10 min (equivalent to precisely 100 observations) measurements were stopped. These last 100 observations were used to compute representative δ^2H and δ^{18}O average values and standard deviations.

2.4. Performance Test and Calibration of the New Method at Different Temperatures

[11] Three working standards were used to conduct the performance test and calibration of the new method at different temperatures: distilled tap water ($\delta^2H_{st1} = -51.86‰ \pm 0.15‰$, $\delta^{18}O_{st1} = -7.69‰ \pm 0.04‰$) and two isotopically enriched waters ($\delta^2H_{st2} = -35.70‰ \pm 0.18‰$, $\delta^{18}O_{st2} = 0.08‰ \pm 0.03‰$, and $\delta^2H_{st3} = 16.79‰ \pm 0.22‰$ $\delta^{18}O_{st3} = 9.06‰ \pm 0.05‰$). All standards were measured at 17,000 ppmv water vapor mixing ratio using the vaporizer unit of the analyzer and an autosampler (number of replicates for each water standard = 4, number of injections per replicate = 8, average and standard deviation calculated without the first three values of the first replicate to account for a potential memory effect of the laser spectrometer). The range of isotopic compositions was similar to those observed in natural soils, i.e., from values of local groundwater to enriched surface water, but excluded cases where snow is present (very negative δ^2H and δ^{18}O). However, the methodology would also be applicable to any other isotopic compositions.

[12] The three vessels were each filled with sand and one of the water standards (standard 1 in vessel 1, standard 2 in vessel 2, standard 3 in vessel 3) until water saturation and were placed in a temperature-controlled water bath. Water vapor was successively sampled from the three vessels on five occasions over a period of 8 weeks at sand temperatures ranging from 8°C to 24°C. This relatively long period was chosen to account for a potential drift of analyzer δ^2H and δ^{18}O values over time and for potential changes of the material properties of the gas-permeable tubing.

2.5. Impact of the Sand Volumetric Water Content and Dry Air Flow Rate on δ^2H_{vap} and $\delta^{18}O_{vap}$

[13] For experiments on the dependence of the new method on sand volumetric water content and dry air flow rate through the gas-permeable tubing, sand temperature was set to 16°C. Via the perforated bottom of the first vessel (filled with distilled tap water, i.e., standard 1), water was withdrawn in four steps, thereby reducing volumetric water content from saturation (0.38 m^3 m^{-3}) down to 0.31, 0.24, 0.17, and 0.09 m^3 m^{-3}, respectively. The withdrawn liquid water was sampled for isotopic analysis to characterize potential changes of δ^2H and δ^{18}O due to isotopic fractionation during water removal. At the five different sand volumetric water content levels, water vapor was sampled from the vessel via the gas-permeable tubing and analyzed following the method described earlier. Finally, sand temperature was reduced to 8°C, and sampling was performed over a period of 4 h to observe potential decreases of water vapor concentration and δ^2H_{vap} and $\delta^{18}O_{vap}$ due to a possibly insufficient supply of water vapor. Additionally, influence of the dry air flow rate on δ^2H_{vap} and $\delta^{18}O_{vap}$ was investigated. For this purpose, soil water vapor was sampled with a dry air flow rate of 100 mL min^{-1} instead of initially 25 mL min^{-1} during 1 h at the end of the 4 h period.

2.6. Monitoring Fast Changes of $\delta^2H_{liq/vap}$ and $\delta^{18}O_{liq/vap}$, and Memory Effect of the Tubing

[14] The objective of this section was to investigate a potential memory effect of the tubing material and whether the new method is suitable to follow fast changes of water isotopic composition over a wide range of δ^2H and δ^{18}O values both in the liquid and in the vapor phase of soils.

[15] For technical reasons (e.g., heterogeneity of the δ^2H_{liq} and $\delta^{18}O_{liq}$ due to preferential flow in the sand during the filling and removing of water), the series of tests for monitoring fast changes of liquid water isotopic composition was performed with pure liquid water. We found that the gas-permeable tubing was not fully waterproof after 2 weeks immersed in pure water. However, the experiments in this section were performed on a much shorter timescale. A vessel containing 0.8 L of distilled tap water (standard 1) with a 1 m piece of gas-permeable tubing immersed in the water was placed in a water bath at 16°C. Consecutively, three portions of 0.2 L each of standard 3 were filled into the vessel until a final volume of 1.4 L was reached. After each addition of water, the water mixture inside the vessel was slowly agitated for 5 min in order to facilitate the homogenization of the isotopically different water standards. Water vapor isotopic composition was monitored before, during, and after water additions, and when the measured δ^2H_{vap} and $\delta^{18}O_{vap}$ had reached steady values, these were compared with the theoretical values obtained from mass balance calculations (MBCs). Theoretical values δ^i_{MBC} (i being for either ^{2}H or ^{18}O) were computed using the following simple two-end mixing equation, considering complete and instantaneous mixing of the waters:

$$\delta^i_{MBC} = \frac{V_m}{(V_m + V_{add})} \times \delta^i_m + \frac{V_{add}}{(V_m + V_{add})} \times \delta^i_{add} \quad (1)$$

with $\delta^i_m, \delta^i_{add}, V_m$, and V_{add} being the isotopic compositions of the liquid water inside the vessel before each addition

and of the added water as well as their respective volumes, respectively. Note that V_{add} was 0.2 L each time.

[16] For testing the suitability of the new method for detecting fast changes in the isotopic composition of water in the vapor phase, another series of tests were performed with water vapor only: the 1 m piece of tubing was placed in an empty vessel immersed in the water bath at a temperature of 16°C. Two dew point generators (LI-610 Portable Dew Point Generator, LI-COR Environmental, USA) set to a dew point temperature of 16°C and filled with water standards 1 and 2, respectively, were used to generate water vapor of different isotopic compositions at a flow rate of 1 L min^{-1} each (Figure 1c). Water vapor from the first dew point generator was run through the vessel. Water vapor isotopic composition inside the vessel was monitored with the gas-permeable tubing (dry air flow rate through the tubing: 25 mL min^{-1}; water vapor mixing ratio in the analyzer: 17,000 ppmv). After δ^2H_{vap} and $\delta^{18}O_{vap}$ values had stabilized, the flow of water vapor through the vessel was switched from the first to the second dew point generator. The changes in isotopic composition of the water vapor in the headspace of the vessel were again measured until values had stabilized.

3. Results

[17] In the following section all linear regression parameters, i.e., slopes and y intercepts, were statistically significant ($p < 0.01$).

3.1. Performance Test and Calibration of the New Method at Different Temperatures

[18] Figure 2 gives an example of water vapor mixing ratios (Figure 2a) and the evolution of δ^2H_{vap} and $\delta^{18}O_{vap}$ (Figures 2b and 2c) values over a measurement cycle at a sand temperature of 14°C (solid lines). Water vapor was sampled successively from the three vessels in ascending order of δ values. In order to observe steady δ^2H_{vap} and $\delta^{18}O_{vap}$, a sampling duration of 30 min for each vessel was needed. Dilution of the sample water vapor with dry air was done manually, which did not always guarantee the water vapor mixing ratio to reach a constant value of 17,000 (±170) ppmv instantaneously. However, during the last 10 min of each 30 min measurement interval the mixing ratio was always stable. The δ^2H_{vap} and $\delta^{18}O_{vap}$ values at thermodynamic equilibrium with sand liquid water calculated from experimental results of *Majoube* [1971] (i.e., $\delta^2H_{vap\_eq}$ and $\delta^{18}O_{vap\_eq}$) are also shown (dashed lines in Figure 2). Isotopic steady state was reached for $\delta^{18}O_{vap}$ in all three vessels, whereas this was not the case for δ^2H_{vap}. Note that the observed difference between δ^2H_{vap} and $\delta^2H_{vap\_eq}$ decreased with increasing δ^2H_{vap}.

[19] Figure 3 shows the dependence of δ^2H_{vap} and $\delta^{18}O_{vap}$ on sand temperatures (solid lines) as well as $\delta^2H_{vap\_eq}$ and $\delta^{18}O_{vap\_eq}$ (dashed lines). The residual standard errors in estimating δ^2H_{vap} and $\delta^{18}O_{vap}$ of all three vessels with a linear regression were only slightly higher than the measurement precision of the laser analyzer for liquid injections, i.e., ranging from 0.05‰ to 0.07‰ for $\delta^{18}O_{vap}$, and from 0.37‰ to 0.60‰ for δ^2H_{vap}. Average values of regression slopes for $\delta^{18}O_{vap}$ and δ^2H_{vap}, i.e., 0.09‰/°C (±0.01‰/°C) and 0.93‰/°C (±0.04‰/°C), respectively, were comparable to those of the theoretical $\delta^{18}O_{vap\_eq}$ and

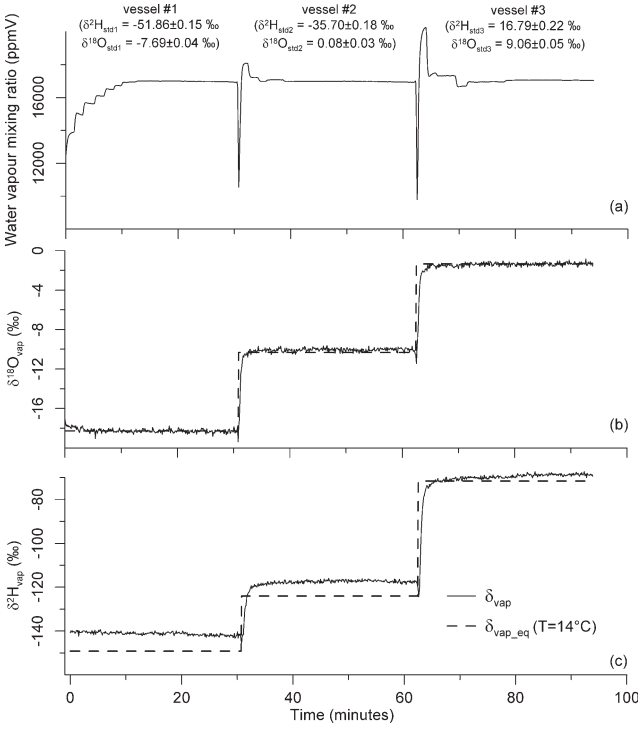

Figure 2. Time course of water vapor mixing ratio, δ^2H_{vap}, and $\delta^{18}O_{vap}$ over a measurement cycle, i.e., from vessel 1 to 3 in ascending order with respect to isotopic ratios. Sand temperature in this experiment was 14°C. The δ^2H_{vap} and $\delta^{18}O_{vap}$ values at thermodynamic equilibrium with liquid water calculated from experimental results of *Majoube* [1971] ($\delta^2H_{vap\_eq}$ and $\delta^{18}O_{vap\_eq}$) are also shown (dashed lines). Values in parentheses are the isotopic signatures of the three standard waters used in the experiments.

$\delta^2H_{vap\_eq}$ and lines, i.e., 0.08‰/°C and 0.96‰/°C. Nevertheless, isotopic steady state was again not reached for δ^2H_{vap} at all tested temperatures, and especially for relatively low δ^2H_{vap} values, i.e., water vapor from vessels 1 and 2 (Figures 3d and 3e), and at low temperature.

[20] Observations of δ^2H_{vap} and $\delta^{18}O_{vap}$ of the three different standards were plotted against the respective measured liquid water isotopic compositions (δ^2H_{liq} and $\delta^{18}O_{liq}$) at a given temperature. Figure 4 displays the slopes and y intercepts of the linear regressions between observed $\delta^{18}O_{vap}$ and δ^2H_{vap} and actual $\delta^{18}O_{liq}$ and δ^2H_{liq} along with their residual standard error (error bars). Regression slopes obtained for the different sand temperatures ranged from 1.069 to 1.075 for δ^2H_{vap} and from 0.998 to 1.004 for $\delta^{18}O_{vap}$. Almost 100% of the variability of $\delta^{18}O_{vap}$ and δ^2H_{vap} y intercepts could be explained by sand temperature. The errors in estimating the y intercepts of $\delta^{18}O_{vap}$ and δ^2H_{vap} were equivalent to the laser analyzer accuracy, i.e., 0.04‰ and 0.44‰, respectively. Finally, the relationships linking δ^2H_{vap} and $\delta^{18}O_{vap}$ to δ^2H_{liq} and $\delta^{18}O_{liq}$ at a given temperature t (°C) were the following:

$$\delta^2H_{liq} = 104.96 - 1.0342*t + 1.0724*\delta^2H_{vap} \quad (2a)$$

$$\delta^{18}O_{liq} = 11.45 - 0.0795*t + 1.0012*\delta^{18}O_{vap} \quad (2b)$$

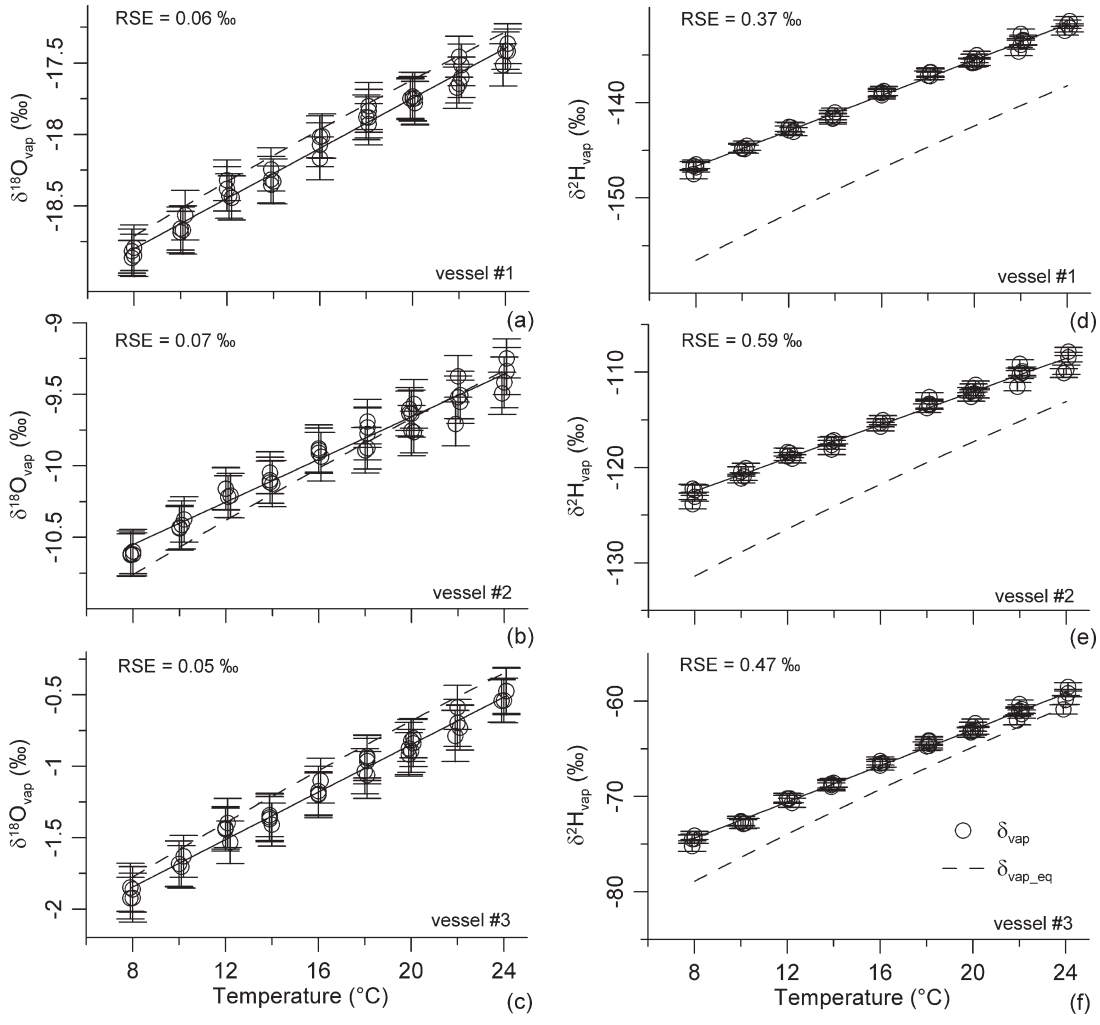

Figure 3. Linear regression relationships (solid lines) of δ^2H_{vap} and $\delta^{18}O_{vap}$ measured with the gas-permeable tubing in the three vessels (symbols) with sand temperature. Theoretical values of δ^2H_{vap} and $\delta^{18}O_{vap}$ at isotopic equilibrium with sand liquid water are represented as well for comparison (dashed lines) [*Majoube*, 1971]. RSE is the residual standard error of the fit to the observed data.

3.2. Influence of Sand Water Content and Dry Air Flow Rate on δ^2H_{vap} and $\delta^{18}O_{vap}$

[21] Analysis of the liquid water removed from the vessel revealed that pumping did not impact the δ^2H_{liq} and $\delta^{18}O_{liq}$ values, i.e., there was no isotopic fractionation during pumping (data not shown), which was a prerequisite of the test. The average δ^2H_{liq} and $\delta^{18}O_{liq}$ values inferred from the vapor measurements between the pumping were −51.69‰ (±0.38‰) and −7.78‰ (±0.11‰), respectively (Figure 5). It shows that sand water content from saturation down to 0.09 $m^3\ m^{-3}$ had no observable influence on the isotope values. At 0.09 $m^3\ m^{-3}$, 8°C sand temperature, and after a sampling period of 4 h, no significant decrease of water vapor concentration in the tubing due to potentially insufficient generation of new water vapor in the sand could be observed. The inferred δ^2H_{liq} and $\delta^{18}O_{liq}$ values at this temperature were also in very good agreement with δ^2H_{st1} and $\delta^{18}O_{st1}$, i.e., −52.19‰ (±0.45‰) and −7.71‰ (±0.14‰), respectively. It was finally observed that at the same conditions a rate of 100 mL min^{-1} of dry air did not affect the calibrated isotope values, with inferred values of $\delta^2H_{liq} = -51.95‰$ (±0.41‰) and $\delta^{18}O_{liq} = -7.85‰$ (±0.15‰).

3.3. Monitoring Fast Changes of $\delta^2H_{liq/vap}$ and $\delta^{18}O_{liq/vap}$ and Memory Effect of the Tubing

[22] Measurements of δ^2H_{vap} and $\delta^{18}O_{vap}$ were carried out continuously before and after the additions of isotopically enriched water in order to determine the time needed to reach the new stable isotope values after the respective water addition. For each step, these values were compared with those obtained by MBCs (equation (1)) for both ^2H and ^{18}O (Figures 6a and 6b). The correlations between measured and calculated values were better for δ^2H than for $\delta^{18}O$, particularly following the second addition of water (i.e., −2.27‰ ± 0.15‰ as opposed to the theoretical value of −2.48‰ for $\delta^{18}O_{liq}$). Time constants (τ) obtained from exponential functions of time ($A\ \exp(-t/\tau) + B$, with A and B being constants and t being the time elapsed after addition of the isotopically different water) fitted to the time course of measured δ^2H_{liq} and $\delta^{18}O_{liq}$ values for each step are reported as well (Figure 6c). Even though the water

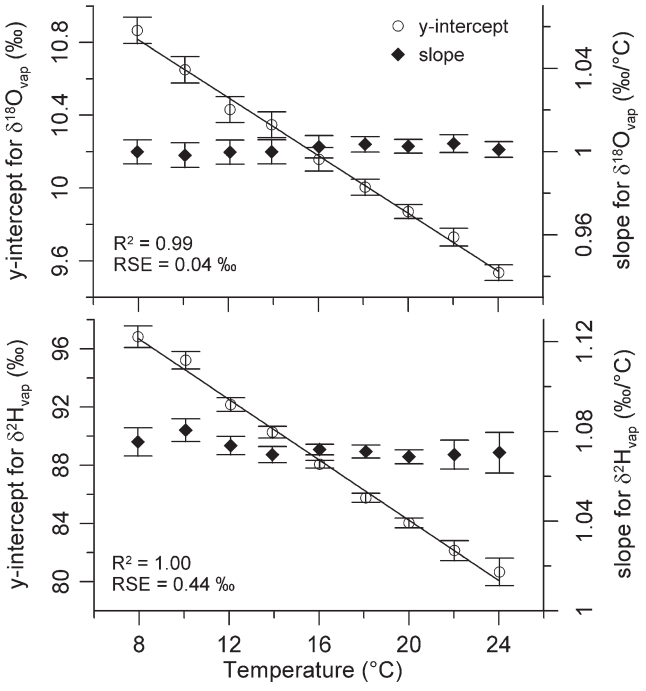

Figure 4. Calibration slope values (black diamonds) and linear regression relationship (solid lines) of the calibration *y*-intercept values (white circles) obtained at the tested temperatures.

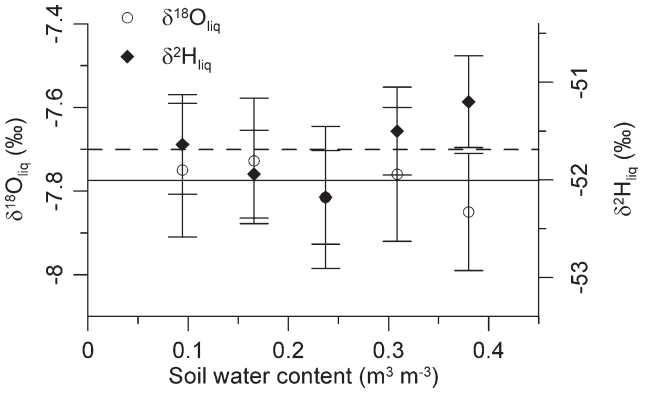

Figure 5. Influence of sand water content on the δ^2H_{liq} and $\delta^{18}O_{liq}$ inferred from the isotopic composition of the water vapor sampled with the gas-permeable tubing. Mean values for δ^2H_{liq} (dashed line) and $\delta^{18}O_{liq}$ (solid line) are reported.

inside the vessel was homogenized after each addition of water, τ ranged between 2.37 and 5.92 h for δ^2H_{liq}, and between 1.12 and 2.58 h for $\delta^{18}O_{liq}$.

[23] In Figure 7, δ^2H_{vap} and $\delta^{18}O_{vap}$ values measured in the headspace of the empty vessel are compared with those of the vapor sampled with the gas-permeable tubing following switching the air flow between the two dew point generators with isotopically different water vapor ($t = 0$ h). The time constant inferred from the evolution of headspace δ^2H_{vap} and $\delta^{18}O_{vap}$ measured without tubing was much smaller (0.45 h) as compared to the experiments with liquid water. The time constants associated with the tubing measurements of δ^2H_{vap} and $\delta^{18}O_{vap}$ were 0.55 h and 1 h, respectively, and thus only marginally longer than without tubing. Whereas initial and final $\delta^{18}O_{vap}$ values in the headspace measured without and with tubing were in good agreement, this was less the case for δ^2H_{vap}, which was slightly enriched in the tubing measurement as compared to measurements without tubing (Figure 7).

4. Discussion

[24] As the three working standards had substantially different δ^2H and $\delta^{18}O$ values, a sampling duration of 30 min was needed when switching between vessels in order to reach stable δ^2H_{vap} and $\delta^{18}O_{vap}$ values. However, under field conditions such large differences in isotopic composition of soil water between different sampling depths may only be observed close to the soil surface at conditions with a strong evaporation flux. Therefore, the sampling duration could be kept substantially lower for deeper soil layers, e.g., a few minutes. For a given temperature within the range tested in this study (8–24°C) a linear relationship was found between observed $\delta^{18}O_{vap}$ and δ^2H_{vap} and actual $\delta^{18}O_{liq}$ and δ^2H_{liq} values that could be used for calibration of the method (equations (2a) and (2b)). Furthermore, the method proved to deliver reproducible results over a period of at least 8 weeks. The fact that the obtained calibration relationships were solely a function of temperature showed that there was no measurable kinetic effect associated with the sampling of soil water vapor. The observed deviation from results of *Majoube* [1971] for ^2H or to other liquid-vapor equilibrium relationships available in the literature (e.g., those of *Bottinga and Craig* [1969], *Kakiuchi and Matsuo* [1979], and *Horita and Wesolowski* [1994]) could not be explained by introducing kinetic fractionation because measured values were enriched relative to the equilibrium values instead of depleted. Enriched δ^2H_{vap} could have been, on the other hand, a result of an enrichment of the soil water close to the tubing due to evaporation occurring in the soil as opposed to pure thermodynamic equilibrium. However, these enriched and steady δ^2H_{vap} values were obtained already after 20 min from the first sampling day on. Moreover, the same values could still be measured after 8 weeks at a given temperature. This cannot be explained by direct application of analytical models describing the time evolution of the isotopic composition of a water body undergoing steady- or transient-state evaporation (e.g., the *Craig and Gordon* [1965] model). With a low dry air flow rate such as 25 mL min^{-1}, it seems that the soil water vapor around the tubing remained still saturated during sampling. Moreover, the length of the gas-permeable tubing allowed its inside air reaching saturation during the last 10 sampling minutes. Water vapor removal therefore occurred for the very most part at thermodynamic equilibrium. This situation is comparable to the so-called Nernst-Bertholet distribution of trace elements between mineral phases as pointed out by *Gat et al*. [1981]. Water vapor removal led in our case to changes of $\delta^{18}O_{liq}$ and δ^2H_{liq} too small to be detectable even after 8 weeks of sampling. The difference observed between the δ^2H_{vap} results of this study and those at equilibrium from the literature could therefore only be due to the permeable tubing material, e.g., potentially a low

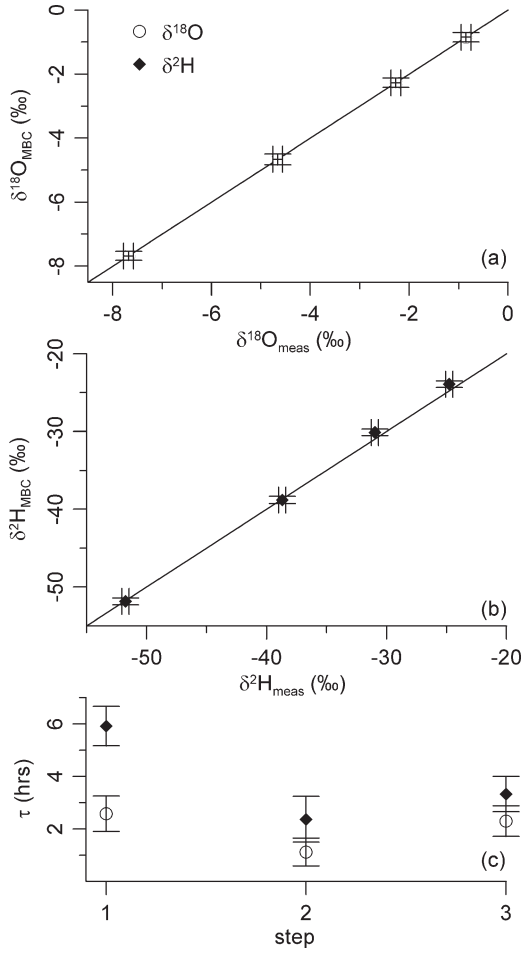

Figure 6. Comparison of δ^2H_{liq} and $\delta^{18}O_{liq}$ final values determined with the gas-permeable tubing immersed in liquid water following stepwise additions of water with a different isotopic composition with those obtained from MBCs. Solid lines are 1:1 lines. The parameter τ is the time constant of an exponential function ($A\ \exp(-t/\tau) + B$; with A and B being constants and t being the time elapsed after addition of the isotopically different water) fitted to the time course of measured δ^2H_{liq} and $\delta^{18}O_{liq}$ values.

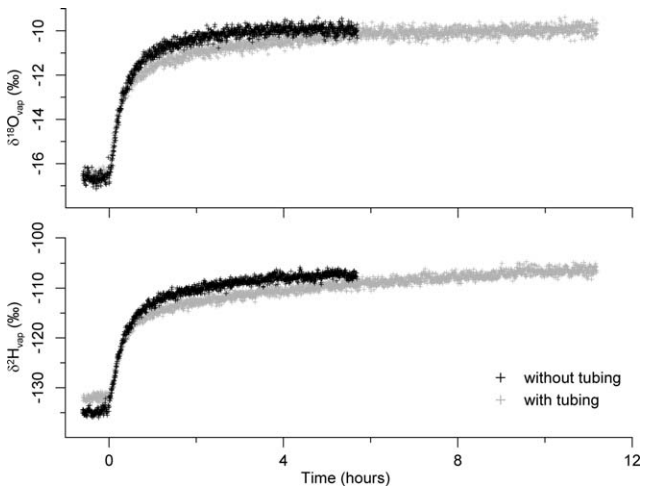

Figure 7. Comparison between δ^2H_{vap} and $\delta^{18}O_{vap}$ measured in the headspace of the vessel without (black crosses) and with the gas-permeable tubing (gray crosses), following a step change of vessel input water vapor isotopic composition ($t = 0$). The vessel air temperature was kept constant at 16°C.

degree of proton exchange between the polypropylene matrix and the water molecules. Finally, the calibration coefficients were obtained with the assumption that the sand was isotopically inert. No exchange of ^2H and ^{18}O could therefore occur between water and the sand matrix leading to eventual fractionation. Like for any other direct-equilibration method [e.g., *Garvelmann et al*., 2012; *Herbstritt et al*., 2012; *Hsieh et al*., 1998; *Scrimgeour*, 1995] or when sampling soil pore water using porous ceramic cups, it is consequently assumed that total and pore water have the same isotopic composition. This may not be true with soils having a very high cation exchange capacity, although corrections to be made have yet to be further investigated (E. Oerter, personal communication).

[25] Even at sand temperatures as low as 8°C and at the lowest sand water content (0.09 $m^3\ m^{-3}$) that could be reached by pumping water from the vessel with a diaphragm pump, there was sufficient water vapor available for the measurements. Moreover, from the 4 h sampling period at 0.09 $m^3\ m^{-3}$ and 8°C, it could be concluded that the volume of water vapor present in the sand was much greater than the volume actually needed for stable measurements of δ^2H_{vap} and $\delta^{18}O_{vap}$ values, i.e., without any changes of δ^2H_{vap} and $\delta^{18}O_{vap}$ values due to isotopic fractionation effects induced by the constant removal of water vapor through the tubing. This was also the case at a much higher dry air flow rate of 100 mL min^{-1} (data not shown). The assumption of water vapor saturation even at low water availability was therefore valid and in agreement with Kelvin's equation linking relative humidity of the soil atmosphere with soil water tension. This relationship states that soil air relative humidity remains higher than 99% from saturation to pF 6 and for temperatures ranging from 0°C to 30°C. Unfortunately, it was not possible to reach water contents below 0.09 $m^3\ m^{-3}$—equivalent to a soil water tension of −0.57 m (pF 1.75)—using the diaphragm vacuum pump setup without withdrawing water vapor and causing isotope fractionation. As the mass flow of saturated water vapor that can be sampled depends on the soil temperature, choosing a low tubing dry air flow rate (such as 25 mL min^{-1} as used in this study) to collect soil water vapor enables the application of the new method even at relatively dry conditions.

[26] The time needed for the permeable tubing to reach the final δ^2H_{vap} and $\delta^{18}O_{vap}$ values when immersed in pure water (i.e., up to a few hours) was considerable in comparison with the almost instantaneous mixing of waters. In the absence of water vapor transport and despite the initial homogenization of the water inside the vessel after each addition, the tubing could not rapidly capture the sudden changes of the δ^2H_{liq} and $\delta^{18}O_{liq}$. A potential explanation of this observation could be that "old" liquid water captured in the micropores of the tubing material had to evaporate first into the tubing before the "new" water with the

different isotopic signature could get in contact with the interior of the tubing. Nevertheless, such fast changes—with the soil remaining at water saturation—are very unlikely to happen in nature, e.g., except for artificial labeling of the ground water. Moreover, the calculated time constants were comparable with most of the measured or modeled liquid hydraulic conductivities of natural soils (i.e., from 10^{-3} to 10^{-7} m s^{-1}). Therefore, we expect our methodology to be applicable under both unsaturated and saturated conditions where temporal changes of δ^2H_{liq} and $\delta^{18}O_{liq}$ values are mainly occurring on a seasonal timescale, for instance, by variation of the isotopic composition of precipitation and of soil temperature.

[27] The experiments with water vapor revealed that the tubing was much more reactive to changes in the isotopic composition than in liquid water. The time constants of measured δ values following a step change in water vapor isotopic composition were almost identical for $\delta^{18}O_{vap}$ and very similar for δ^2H_{vap} for measurements with and without tubing. Interestingly, and as observed during the calibration, there was a slight ^2H enrichment of the tubing water vapor as compared to the value at equilibrium calculated according to *Majoube* [1971]. Moreover, these differences were greater at low δ^2H_{vap} ($\Delta\delta^2H_{vap} = \sim 3‰$) than at high δ^2H_{vap}, i.e., at the end of the sampling period ($\Delta\delta^2H_{vap} = \sim 1.5‰$) at a temperature of 16°C.

[28] From the two last experiments, it can be inferred that a memory effect associated with the tubing material as well as with the sampling methodology is only relevant for applications in water-saturated soils, whereas it does not play a significant role in the unsaturated zone of the soil, where water vapor transport plays the dominating role in determining the isotopic composition of the soil water. Nevertheless, the new method is also applicable at water-saturated conditions, as its time constant for observing changes in isotopic composition of soil water is compatible with the temporal variations observed in nature.

[29] Our method is deployable in the field (given that electricity and a shelter for the instrument are available) and applicable to a wide range of conditions. Tests demonstrated that the gas-permeable tubing could withstand fully saturated conditions in soil and even oversaturated conditions for more than 2 weeks which makes it suitable during heavy rain events (e.g., ponding and surface runoff). There are different possibilities for the installation of the permeable tubing. One of them would be to excavate two soil pits separated by 1 m and insert from one to the other the piece of gas-permeable tubing fixed to a 0.9 cm diameter auger horizontally in the soil. Both ends of the tubing are then connected to the laser spectrometer with isolated inert flexible or metal pipes. Each measurement depth should have its separate and independent section of tubing. The top of the soil profile (approximately the first 20 cm) should be equipped with as many tubing sections as possible to better characterize its dynamics with high vertical resolution. At the soil surface, the tubing simply is to be buried. Finally, potential users should note that monitoring of the δ^2H_{liq} and $\delta^{18}O_{liq}$ in natural soils using our method can be performed at any level of water vapor mixing ratio, provided that a prior characterization of their laser spectrometer's dependence on this variable has been made (e.g., according to the method of *Schmidt et al*. [2010]).

5. Conclusion

[30] This study demonstrates for the first time that soil δ^2H_{liq} and $\delta^{18}O_{liq}$ can be monitored nondestructively with high time resolution by combining infrared laser spectrometry for direct measurements of δ^2H_{vap} and $\delta^{18}O_{vap}$ with a specific polypropylene tubing permeable to water vapor. This was possible at the condition of a prior calibration of the measured δ^2H_{vap} and $\delta^{18}O_{vap}$ against the actual δ^2H_{liq} and $\delta^{18}O_{liq}$ at given temperatures. Although the measured sand δ^2H_{vap} showed a significant enrichment relative to those determined at equilibrium according to *Majoube* [1971] at all tested temperatures, this could be linearly corrected for. Our method can be applied in the field to monitor entire soil profiles as only 1 m of tubing, and a temperature sensor is needed for each sampling depth to sample water vapor and derive the corresponding δ^2H_{liq} and $\delta^{18}O_{liq}$ values. A dry air flow rate of 25 mL min^{-1} allows collecting water vapor without impacting the δ^2H_{liq} and $\delta^{18}O_{liq}$ from saturation down to a soil water tension of at least −57 cm for a temperature range of at least 8°C–24°C. Finally, the rapidity at which the tubing is able to detect changes of δ^2H_{liq} and $\delta^{18}O_{liq}$ is suitable for the great majority of transport properties in natural soils.

[31] **Acknowledgments.** This study was conducted in the framework of and with means from the Bioeconomy Portfolio Theme of the Helmholtz Association of German Research Centers. The authors would like to thank Holger Wissel and Andreas Lücke for technical support and Lutz Weihermüller for providing the sand and helping with designing the acrylic glass cylinders. Special thanks go to the Institute of Meteorology and Climate Research (IMK-IFU), Karlsruhe Institute of Technology, for providing the water isotopic analyzer for this study.

References

Berman, E. S. F., M. Gupta, C. Gabrielli, T. Garland, and J. J. McDonnell (2009), High-frequency field-deployable isotope analyzer for hydrological applications, *Water Resour. Res.*, *45*, W10201, doi:10.1029/2009WR008265.

Bottinga, Y., and H. Craig (1969), Oxygen isotope fractionation between CO_2 and water and isotopic composition of marine atmospheric CO_2, *Earth Planet. Sci. Lett.*, *5*(5), 285–&.

Craig, H., and L. I. Gordon (1965), *Deuterium and oxygen 18 variations in the ocean and marine atmosphere, paper presented at Stable Isotopes in Oceanographic Studies and Paleotemperatures*, V. Lishi, Spoleto, Italy.

Dinsmore, K. J., M. F. Billett, and T. R. Moore (2009), Transfer of carbon dioxide and methane through the soil-water-atmosphere system at Mer Bleue peatland, Canada, *Hydrol. Processes*, *23*, 330–341, doi:10.1002/hyp.7158.

Garvelmann, J., C. Kulls, and M. Weiler (2012), A porewater-based stable isotope approach for the investigation of subsurface hydrological processes, *Hydrol. Earth Syst. Sci.*, *16*(2), 631–640, doi:10.5194/hess-16–631-2012.

Gat, J. R., R. Gonfiantini, J. C. Fontes, B. Árnason, P. Fritz, M. Magaritz, C. Panichi, B. R. Payne, and Y. Yurtsever (1981), Stable isotope hydrology. Deuterium and oxygen-18 in the water cycle, *Rep. 210*, *337 pp*, IAEA, Vienna, Austria.

Gonfiantini, R. (1978), Standards for stable isotope measurements in natural compounds, *Nature*, *271*, 534–536.

Griffis, T. J., et al. (2010), Determining the oxygen isotope composition of evapotranspiration using eddy covariance, *Boundary-Layer Meteorol.*, *137*, 307–326, doi:10.1007/s10546-010-9529-5.

Hartmann, A. A., N. Buchmann, and P. A. Niklaus (2011), A study of soil methane sink regulation in two grasslands exposed to drought and N fertilization, *Plant Soil*, *342*(1–2), 265–275, doi:10.1007/s11104-010-0690-x.

Haverd, V., and M. Cuntz (2010), Soil-Litter-Iso: A one-dimensional model for coupled transport of heat, water and stable isotopes in soil with a litter layer and root extraction, *J. Hydrol.*, *388*, 438–455.

Helliker, B. R., and D. Noone (2010), Novel approaches for monitoring of water vapor isotope ratios: Plants, lasers and satellites, in *Isoscapes—Understanding Movement, Pattern, and Process on Earth Through Isotope Mapping*, edited by J. B. West et al., pp. 71–88, Springer, New York.

Herbstritt, B., B. Gralher, and M. Weiler (2012), Continuous in situ measurements of stable isotopes in liquid water, *Water Resour. Res.*, *48*, W03601, doi:10.1029/2011wr011369.

Horita, J., and D. J. Wesolowski (1994), Liquid-vapor fractionation of oxygen and hydrogen isotopes of water from the freezing to the critical temperature, *Geochim. Cosmochim. Acta*, *58*, 3425–3437.

Hsieh, J. C. C., O. A. Chadwick, E. F. Kelly, and S. M. Savin (1998), Oxygen isotopic composition of soil water: Quantifying evaporation and transpiration, *Geoderma*, *82*(1–3), 269–293, doi:10.1016/S0016-7061(97)00105-5.

Iannone, R. Q., D. Romanini, O. Cattani, H. A. J. Meijer, and E. R. T. Kerstel (2010), Water isotope ratio (d2H and d18O) measurements in atmospheric moisture using an optical feedback cavity enhanced absorption laser spectrometer, *J. Geophys. Res.*, *115*, D10111, doi:10.1029/2009JD012895.

Kakiuchi, M., and S. Matsuo (1979), Direct measurements of D-H and O-18-O-16 fractionation factors between vapor and liquid water in the temperature-range from 10 to 40-degrees-C, *Geochem. J.*, *13*(6), 307–311.

Kerstel, E. R. T., R. van Trigt, N. Dam, J. Reuss, and H. A. J. Meijer (1999), Simultaneous determination of the 2H/1H, 17O/16O, and 18O/16O isotope abundance ratios in water by means of laser spectrometry, *Anal. Chem.*, *71*, 5297–5303, doi:10.1021/ac990621e.

Lambot, S., E. Slobc, J. Rhebergend, O. Loperaa, K. Z. Jadoona, and H. Vereecken (2009), Remote estimation of the hydraulic properties of a sand using full-waveform integrated hydrogeophysical inversion of time-lapse, off-ground GPR data, *Vadoze Zone J.*, *8*, 743–754, doi:10.2136/vzj2008.0058.

Luz, B., E. Barkan, R. Yam, and A. Shemesh (2009), Fractionation of oxygen and hydrogen isotopes in evaporating water, *Geochim. Cosmochim. Acta*, *73*, 6697–6703.

Majoube, M. (1971), Fractionnement en oxygène-18 et en deuterium entre l'eau et sa vapeur, *J. Chem. Phys.*, *68*, 1423–1436.

Martinelli, L. A., R. L. Victoria, L. S. L. Sternberg, A. Ribeiro, and M. Z. Moreira (1996), Using stable isotopes to determine sources of evaporated water to the atmosphere in the Amazon basin, *J. Hydrol.*, *183*, 191–204.

Moreira, M. Z., L. d. S. L. Sternberg, L. A. Martinelli, R. L. Victoria, E. M. Barbosa, L. C. M. Bonates, and D. C. Nepstad (1997), Contribution of transpiration to forest ambient vapour based on isotopic measurements, *Global Change Biol.*, *3*, 439–450.

Neftel, A., A. Blatter, M. Schmid, B. Lehmann, and S. V. Tarakanov (2000), An experimental determination of the scale length of N_2O in the soil of a grassland, *J. Geophys. Res.*, *105*(D10), 12,095–12,103, doi:10.1029/2000JD900088.

Rothfuss, Y., P. Biron, T. Bariac, I. Braud, L. Canale, J. L. Durand, J. P. Gaudet, P. Richard, and M. Vauclin (2010), Partitioning evapotranspiration fluxes into soil evaporation and plant transpiration using water stable isotopes under controlled conditions, *Hydrol. Processes*, *24*, 3177–3194.

Rothfuss, Y., I. Braud, N. Le Moine, P. Biron, J. L. Durand, M. Vauclin, and T. Bariac (2012), Factors controlling the isotopic partitioning between soil evaporation and plant transpiration: Assessment using a multi-objective calibration of SiSPAT-Isotope under controlled conditions, *J. Hydrol.*, *442*, 75–88, doi: 10.1016/j.jhydrol.2012.03.041.

Schmidt, M., K. Maseyk, C. Lett, P. Biron, P. Richard, T. Bariac, and U. Seibt (2010), Concentration effects on laser-based $\delta^{18}O$ and $\delta^{2}H$ measurements and implications for the calibration of vapour measurements with liquid standards, *Rapid Commun. Mass Spectrom.*, *24*, 3553–3561, doi:10.1002/rcm.4813.

Scrimgeour, C. M. (1995), Measurement of plant and soil-water isotope composition by direct equilibration methods, *J. Hydrol.*, *172*(1–4), 261–274, doi:10.1016/0022-1694(95)02716-3.

Singleton, M. J., E. L. Sonnenthal, M. E. Conrad, D. J. DePaolo, and W. Glendon (2004), Multiphase reactive transport modeling of seasonal infiltration events and stable isotope fractionation in unsaturated zone pore water and vapor at the Hanford site, *Vadoze Zone J.*, *3*, 775–785.

Wang, P., X. Song, D. Han, Y. Zhang, and X. Liu (2010), A study of root water uptake of crops indicated by hydrogen and oxygen stable isotopes: A case in Shanxi Province, China, *Agric. Water Manage.*, *97*, 475–482.

Webster, C. R., and A. J. Heymsfield (2003), Water isotope ratios D/H, 18O/16O, 17O/16O in and out of clouds map dehydration pathways, *Science*, *302*, 1742–1745, doi:10.1126/science.1089496.

Williams, D. G., et al. (2004), Evapotranspiration components determined by sable isotope, sap flow and eddy covariance techniques, *Agric. For. Meteorol.*, *125*, 241–258.

Yakir, D., and L. D. L. Sternberg (2000), The use of stable isotopes to study ecosystem gas exchange, *Oecologia*, *123*(3), 297–311, doi:10.1007/s004420051016.

Yepez, E. A., D. G. Williams, R. L. Scott, and G. Lin (2003), Partitioning overstory and understory evapotranspiration in a semiarid savanna woodland from the isotopic composition of water vapour, *Agric. For. Meteorol.*, *119*, 53–68.

Yepez, E. A., T. E. Huxman, D. D. Ignace, N. B. English, J. F. Weltzin, A. E. Castellanos, and D. G. Williams (2005), Dynamics of transpiration and evaporation following a moisture pulse in semirarid grassland: A chamber-based isotope methods for partitioning flux components, *Agric. For. Meteorol.*, *132*, 359–376.